PCCP

COMMUNICATION

View Article Online
View Journal | View Issue

Cite this: *Phys. Chem. Chem. Phys.*, 2019, **21**, 12087

Received 16th April 2019,
Accepted 17th May 2019

DOI: 10.1039/c9cp01052a

rsc.li/pccp

Tuning the liquid-phase exfoliation of arsenic nanosheets by interaction with various solvents†

Zheng-Hang Qi,‡ Yi Hu,‡ Zhong Jin * and Jing Ma *

The interaction between monolayered arsenene and fourteen kinds of solvents is found to be correlated with the extent of charge transfer from arsenene to the solvents by density functional theory calculations. Among them, three kinds of aprotic solvents (cyclohexane, tetrahydrofuran and chloroform), representing different adsorbability with arsenene, were selected to exfoliate bulk arsenic crystals into nanosheets in experiments. The as-prepared concentrations of the three dispersions vary monotonically with the calculated adsorption energies and charge transfer per contact area. Transmission electron microscopy (TEM) characterization and size distribution analyses manifested that the lateral size distributions of the exfoliated arsenic nanosheets ranged from 100 nm to 1050 nm. This strategy shows the potential usage in liquid-phase exfoliation of multi-layered materials due to the interaction effects between the solvents and the surface of the materials.

Two-dimensional (2D) materials have garnered tremendous interest over the past few years because of their unique electronic properties and high specific surface areas which are important in diverse technologies, including electronics, optoelectronics and catalysis. In the family of 2D materials, group-VA members have shown increasing research interest, strong momentum of development and promising applications.[1,2] As a novel type of promising 2D materials, group-VA arsenene has been drawing more and more attention. Intensive theoretical studies on pristine or functionalized arsenene have been reported, which predicted unique and multifarious properties.[3–15] However, the exfoliation of bulk arsenic into few-layered arsenene still faces huge obstacles to date. Since the successful exfoliation of graphite into single atomic layers of graphene by Geim and Novoselov in 2004,[16] different production methods for 2D materials have been developed including mechanical exfoliation, chemical vapour deposition, chemical exfoliation, and liquid-phase exfoliation. In particular, liquid-phase exfoliation is well-known as a convenient and cost-effective option to prepare 2D materials without intermediate chemical reactions.[17] Very recently, Pumera *et al.* and Rao *et al.* successfully employed liquid-phase exfoliation to the preparation of arsenene nanosheets.[18,19] Despite the successful application of liquid-phase exfoliation in the preparation of a few mono- to few-layered 2D materials, a number of intrinsic characteristics are still to be elucidated. In particular, the interactions between 2D materials and solvents should be further understood.

Herein, we identified a correlation between the adsorption energies and charge transfer of solvents on arsenene by means of density functional theory (DFT) calculations. The calculated adsorption energies vary with the charge transfer value nearly linearly for the aprotic solvents. The experiments of liquid-phase exfoliation for several selected aprotic solvents further supported their potential usage in liquid-phase exfoliation of multi-layered materials by the high-throughput screening of interaction effects between the solvents and the surface of the materials.

The initial study of liquid-phase exfoliation of arsenene starts with the screening of solvents by using DFT computations of interaction energies between the chosen solvents and arsenene. The chosen solvents could be divided into two categories: aprotic solvents and protic solvents (Fig. 1a). The solvents are all common commercial products that were chosen based on their physical properties. For example, the dielectric constants of the chosen solvents range from 1.9 (hexane) to 78.4 (water) and the values of pK_a are between 3.8 (formic acid) and 15.5 (methanol and ethanol) for the protic solvents (Table S1, ESI†). Different types of solvents with the same category were also taken into consideration such as the linear alkane (hexane), cyclic alkane (cyclohexane), aromatic compound (benzene), ether compound (tetrahydrofuran) and so on. Previous studies have found that solvents with high boiling points work particularly well in the liquid exfoliation of graphene such as *N*-methylpyrrolidone and *N*,*N*-dimethylformamide.[20,21]

Key Laboratory of Mesoscopic Chemistry of MOE, Jiangsu Key Laboratory of Advanced Organic Materials, School of Chemistry & Chemical Engineering, Nanjing University, 22 Hankou Road, Nanjing, 210093, People's Republic of China. E-mail: majing@nju.edu.cn, zhongjin@nju.edu.cn

† Electronic supplementary information (ESI) available. See DOI: 10.1039/c9cp01052a

‡ These authors contributed equally.

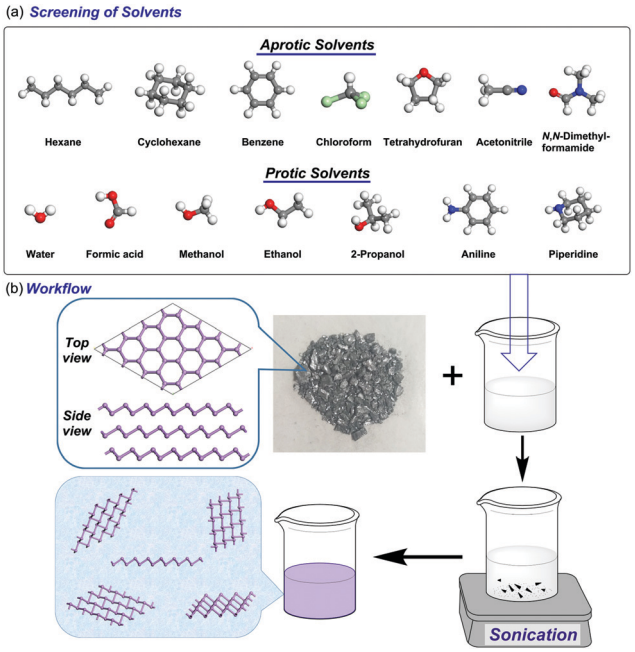

Fig. 1 Schematic description of the screening of solvents for liquid-phase exfoliation of arsenene. (a) Aprotic solvents and protic solvents. (b) Workflow of liquid-phase exfoliation.

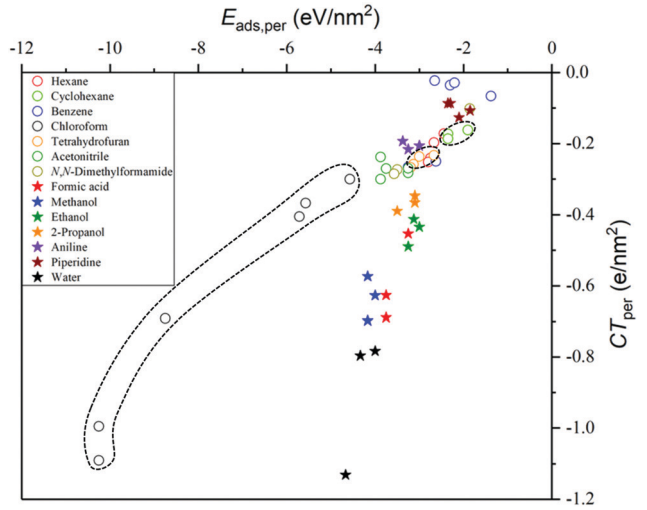

Fig. 2 Plot of adsorption energy per unit area ($E_{ads,per}$) *versus* charge transfer per unit area (CT_{per}) in different solvents. The circles are aprotic and the stars are protic solvents. The solvents with dashed circles were selected for liquid-phase exfoliation experiments.

However, the high-boiling point solvents are difficult to remove and will cause trouble in the following processing. Thus, low-boiling point solvents with comparable performance are desired.

The monolayer model of gray arsenic adopts a buckled structure (Fig. 1b), which is derived from fully optimized pristine arsenene with the lattice constant of 3.607 Å and the As–As bond length of 2.517 Å, in good agreement with previous reports.[2,4,6]

To estimate the interaction intensity between arsenene and solvents, adsorption energies were calculated by DFT. The adsorption energy is defined by the formula: $E_{ads} = E_{total} - E_{As} - E_{sol}$, where E_{total} is the total energy of arsenene with adsorbed solvent and E_{As} and E_{sol} are individual energies of the pristine arsenene and isolated solvent, respectively. For most solvents, similar adsorption energies can be observed regardless of the different adsorption sites and orientations of the solvents relative to the substrate (Scheme S1, ESI†). All the negative adsorption energies indicate the attractive noncovalent interactions, which are common in the adsorption of molecules on the surface of materials.

The extent of charge transfer, *i.e.*, the difference in charge between pristine arsenene and the arsenene–solvent complex, was estimated by Bader charge analysis and its value reflects the amount of change in the valence electron of arsenene. It is worth noting that all the values of the charge transfer are also negative, which means that arsenene acts as the electron donor and transfers charge to the solvent molecules. This implies that arsenene is a type of strong electron-rich 2D materials. The plot (Fig. S1, ESI†) of adsorption energy *versus* charge transfer shows a linear relation for aprotic solvents with some exceptions. Nevertheless, the relation between adsorption energies and charge transfer is disordered to some extent for protic solvents. From the plot, it could be inferred that, in general, more charge is transferred from arsenene to the solvent, and the adsorption is energetically more favourable.

In order to compare the interactions between arsenene and different solvents under the same conditions, the contact area of the solvent on arsenene was estimated (Scheme S3, ESI†). The adsorption energies and values of charge transfer per unit area were calculated as shown in Fig. 2. It is worth noting that multiple geometries were calculated for each solvent, so there are multiple circles/stars for each compound. This treatment aims to simulate the real situation as much as possible because arsenene is fully covered by solvent molecules in the solution. Undoubtedly, the linear relation remains due to the simultaneous expansion or shrinkage of the *x*- and *y*-axis values for each point of aprotic solvents. What's interesting is that a linear relation seems to appear for protic solvents too. Generally, the points of protic solvents are below those of the aprotic solvents. This is mainly due to the positively charged hydrogen in the protic solvents. From these points, we could select the appropriate solvents to perform the experiments concerned with the surface of arsenene, such as the liquid-phase exfoliation of arsenic nanosheets. The net energetic cost is a fundamental reference in the liquid-phase exfoliation.[22] Strong solvent–solute interactions are anticipated to facilitate the exfoliation effectively.[23]

Stimulated by the theoretical results, three low-boiling point aprotic solvents (cyclohexane, tetrahydrofuran and chloroform) were selected to perform the liquid-phase exfoliation experiments. Photographs of arsenic nanosheet dispersions in chloroform (left), tetrahydrofuran (middle) and cyclohexane (right) after 1000 rpm (90*g*, g = 9.8 m s^{-2}) centrifugation for 5 min are shown in Fig. 3a. The colour variations of the dispersions are related to the concentration of arsenic nanosheets, which strongly depends on the interaction between arsenene and the solvents. The concentrations of the three dispersions were

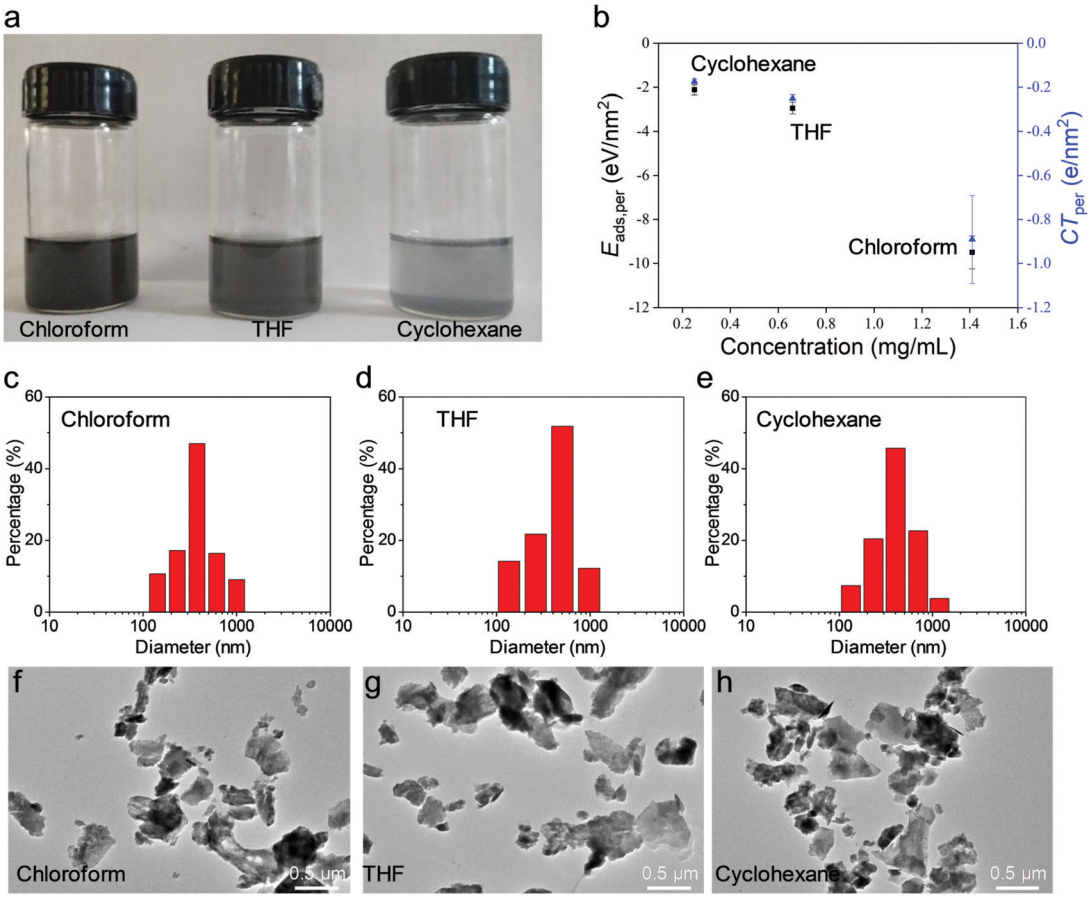

Fig. 3 Yields, size distributions and TEM characterizations of arsenic nanosheets exfoliated in chloroform, tetrahydrofuran (THF) and cyclohexane, respectively.

calculated to be 1.41 mg mL^{-1} in chloroform, 0.66 mg mL^{-1} in tetrahydrofuran and 0.25 mg mL^{-1} in cyclohexane, respectively. $E_{ads,per}$ (black square) and CT_{per} (blue triangle), as the functions of the concentration for arsenic nanosheets, show that the concentrations of the arsenic nanosheet dispersions are associated with $E_{ads,per}$ and CT_{per}. The absolute values of $E_{ads,per}$ and CT_{per} increase nearly monotonically with the concentration of exfoliated arsenic nanosheets (Fig. 3b). Fig. 3c–e illustrate the size distribution of arsenic nanosheets determined by dynamic light scattering. The nanosheets were exfoliated *via* sonication in chloroform, tetrahydrofuran and cyclohexane, respectively, and re-dispersed in ethyl alcohol. No obvious difference in the size distributions was observed. Transmission electron microscopy (TEM) characterizations of arsenic nanosheets exfoliated in chloroform, tetrahydrofuran and cyclohexane are shown in Fig. 3f–h. The three TEM images show typical characteristics of nanosheets, confirming the successful exfoliation of layered arsenic crystals. Atomic force microscopy (AFM) characterization was also performed to estimate the thickness of the exfoliated samples. As shown in Fig. S5 (ESI†), the AFM height profiles show that the thickness values range from 33 to 49 nm. The chemical quality of the solvent-exfoliated samples was assessed *via* XPS as shown in Fig. S7 (ESI†). The XPS spectra have weak As–O sub-bands resulting from trace amounts of oxidation in the samples. The lower XPS signal intensity of As–O indicates only slight oxidation and relatively high stability of the exfoliated samples.

It is necessary and important to evaluate the cytotoxicity of the arsenic nanosheets produced by our method for extending the applications in arsenic mineral resource utilization and biomedical fields. A Cell Counting Kit (CCK-8) assay against 3T3 cells (3 day transfer, inoculum 3×10^5 cells of mouse embryonic fibroblast cells) was performed. As one of the popular techniques for evaluating *in vitro* cell viability, the CCK-8 assay results of arsenene exfoliated in chloroform are shown in Fig. 4a, in comparison with those of pure chloroform solvent (Fig. 4b). The nanosheets exfoliated in other solvents (THF and cyclohexane) were also tested (Fig. S8 and S9, ESI†). After 24 hours in cell culture media, it displayed that almost no cell viability inhibition was detected with low concentrations. No obvious cytotoxicity was observed until the concentration of the nanosheets exfoliated in chloroform reaches 20 μg mL^{-1}. The experimental results indicate that the arsenic nanosheets produced by our method may be applicable to biosensors and biomedical devices in the future.

In conclusion, a relation was found between adsorption energies and charge transfer for solvent-adsorbed arsenene. For aprotic solvents, the adsorption energies vary with the

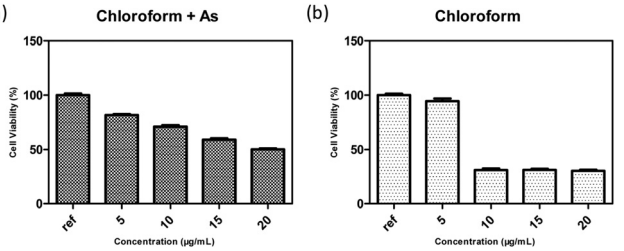

Fig. 4 Percentage cell viability with different concentrations of (a) a mixture of arsenic nanosheets and chloroform and (b) pure chloroform.

charge transfer value almost linearly. The protic solvents tend to gain more charge from arsenene compared to aprotic solvents. Three low-boiling point aprotic solvents (cyclohexane, tetrahydrofuran and chloroform) were selected to perform the liquid-phase exfoliation experiments. The experiments further supported the potential usage in liquid-phase exfoliation of multi-layer materials. It was also found that arsenic nanosheets exfoliated by our method show low toxicity to 3T3 cells, which implies potential application in biosensors and biomedical devices. Together with experimental probes, this shows an example of how computations promote experiments in the liquid-phase exfoliation of arsenic nanosheets. We anticipate that more computational techniques will be involved in developing novel 2D materials.

This work was supported by the National Key Research and Development Program of China (2017YFB0702600 and 2017YFB0702601), and the National Natural Science Foundation of China (Grant No. 21673111 and 21873045). We are grateful to the High Performance Computing Center of Nanjing University for performing the quantum chemical calculations in this communication on its IBM Blade cluster system.

Conflicts of interest

There are no conflicts to declare.

References

1 S. Zhang, S. Guo, Z. Chen, Y. Wang, H. Gao, J. Gómez-Herrero, P. Ares, F. Zamora, Z. Zhu and H. Zeng, *Chem. Soc. Rev.*, 2018, **47**, 982–1021.
2 M. Pumera and Z. Sofer, *Adv. Mater.*, 2017, **29**, 1605299.
3 S. Zhang, Z. Yan, Y. Li, Z. Chen and H. Zeng, *Angew. Chem., Int. Ed.*, 2015, **54**, 3112–3115.
4 J. Zhao, Z.-H. Qi, Y. Xu, J. Dai, X. C. Zeng, W. Guo and J. Ma, *Wiley Interdiscip. Rev.: Comput. Mol. Sci.*, 2018, **8**, e1387.
5 C. Kamal and M. Ezawa, *Phys. Rev. B: Condens. Matter Mater. Phys.*, 2015, **91**, 085423.
6 L. Kou, Y. Ma, X. Tan, T. Frauenheim, A. Du and S. Smith, *J. Phys. Chem. C*, 2015, **119**, 6918–6922.
7 J. Zhao, Y. Li and J. Ma, *Nanoscale*, 2016, **8**, 9657–9666.
8 J. Zhao, W. Guo and J. Ma, *Nano Res.*, 2017, **10**, 491–502.
9 J. Du, C. Xia, Y. An, T. Wang and Y. Jia, *J. Mater. Sci.*, 2016, **51**, 9504–9513.
10 X. Sun, Y. Liu, Z. Song, Y. Li, W. Wang, H. Lin, L. Wang and Y. Li, *J. Mater. Chem. C*, 2017, **5**, 4159–4166.
11 S. Zhang, M. Xie, F. Li, Z. Yan, Y. Li, E. Kan, W. Liu, Z. Chen and H. Zeng, *Angew. Chem., Int. Ed.*, 2016, **55**, 1666–1669.
12 R. Gusmão, Z. Sofer, D. Bouša and M. Pumera, *Angew. Chem., Int. Ed.*, 2017, **56**, 14417–14422.
13 F. Xia, S. Xiong, Y. He, Z. Shao, X. Zhang and J. Jie, *J. Phys. Chem. C*, 2017, **121**, 19530–19537.
14 D. Singh, S. K. Gupta, Y. Sonvane and S. Sahoo, *Nanotechnology*, 2017, **28**, 495202.
15 N. Gao, Y. F. Zhu and Q. Jiang, *J. Mater. Chem. C*, 2017, **5**, 7283–7290.
16 K. S. Novoselov, A. K. Geim, S. V. Morozov, D. Jiang, Y. Zhang, S. V. Dubonos, I. V. Grigorieva and A. A. Firsov, *Science*, 2004, **306**, 666–669.
17 H. Tao, Y. Zhang, Y. Gao, Z. Sun, C. Yan and J. Texter, *Phys. Chem. Chem. Phys.*, 2017, **19**, 921–960.
18 S. M. Beladi-Mousavi, A. M. Pourrahimi, Z. Sofer and M. Pumera, *Adv. Funct. Mater.*, 2019, **29**, 1807004.
19 P. Vishnoi, M. Mazumder, S. K. Pati and C. N. R. Rao, *New J. Chem.*, 2018, **42**, 14091–14095.
20 J. N. Coleman, M. Lotya, A. O'Neill, S. D. Bergin, P. J. King, U. Khan, K. Young, A. Gaucher, S. De, R. J. Smith, I. V. Shvets, S. K. Arora, G. Stanton, H.-Y. Kim, K. Lee, G. T. Kim, G. S. Duesberg, T. Hallam, J. J. Boland, J. J. Wang, J. F. Donegan, J. C. Grunlan, G. Moriarty, A. Shmeliov, R. J. Nicholls, J. M. Perkins, E. M. Grieveson, K. Theuwissen, D. W. McComb, P. D. Nellist and V. Nicolosi, *Science*, 2011, **331**, 568–571.
21 A. O'Neill, U. Khan, P. N. Nirmalraj, J. Boland and J. N. Coleman, *J. Phys. Chem. C*, 2011, **115**, 5422–5428.
22 Y. Hernandez, V. Nicolosi, M. Lotya, F. M. Blighe, Z. Sun, S. De, I. T. McGovern, B. Holland, M. Byrne, Y. K. Gun'Ko, J. J. Boland, P. Niraj, G. Duesberg, S. Krishnamurthy, R. Goodhue, J. Hutchison, V. Scardaci, A. C. Ferrari and J. N. Coleman, *Nat. Nanotechnol.*, 2008, **3**, 563–568.
23 Y. Hernandez, M. Lotya, D. Rickard, S. D. Bergin and J. N. Coleman, *Langmuir*, 2010, **26**, 3208–3213.